

Robust Attitude Control with Fuzzy Momentum Unloading for Satellites Using Reaction Wheels

J. Zapf*

Dept. of Electrical & Computer Engineering
Purdue School of Engineering & Tech., IUPUI
Indianapolis, IN 46202
jjzapf@iupui.edu

Abstract

Keywords: attitude control, robust control, fuzzy logic

The performance and power characteristics of any satellite attitude control system are crucial to the success of the satellite mission. This is especially true for small satellites, which have some of the strictest constraints of all. Reaction wheel systems are an attractive means of control for many satellites, because they offer a high pointing accuracy and are not fuel dependent. These systems are typically more complex, however, and can be fairly demanding on the satellite power system. This paper focuses on two major difficulties associated with the implementation of reaction wheel systems. First, the problem of model uncertainty and system robustness is addressed. In this portion of the paper, the equations of attitude dynamics are linearized with respect to the target attitude and robust control theory is used to ensure robust stability against parametric uncertainty in the reaction wheel angular momentum and satellite inertia matrix. Second, the problem of momentum unloading via induced magnetism is addressed. In this portion of the paper, a fuzzy gain-scheduler is developed to better utilize available resources and minimize power consumption during critical satellite functions.

1 Introduction

The simulations and attitude control strategies discussed in the remainder of this paper were originally developed in support of the Thunderstorm Effects in Space Technology (TEST) Nanosatellite project. TEST is a 30 Kg scientific nanosatellite developed at Taylor University through the University Nanosat Pro-

gram sponsored by the Air Force Office of Space Research. As its name indicates, the intent of the TEST program was to study a variety phenomena associated with thunderstorm activity in the upper atmosphere.



Figure 1: TEST Nanosatellite

Two of the instruments on board the TEST Nanosatellite are a CCD limb-imaging camera and a Hertzberg photometer. System constraints on these instruments required that the satellite maintain an attitude consistent with the local-vertical/local-horizontal (LVLH) frame. Specifically, the camera was constrained to point 20 degrees below the horizon with an accuracy of approximately ± 1 degree and the photometer was constrained to point in as near a nadir direction as possible. Furthermore, TEST houses a variety of plasma instruments that require a specific, although less stringent, orientation, placing yet additional constraints on the attitude system.

To meet these requirements it was determined that TEST should employ an active means of attitude stabilization. Magnetic stabilization methods were initially considered, but were determined to be insufficient for the satellite's mission objectives. Thus, it was decided that a reaction wheel system should be used as

*The author is a graduate student in the M.S. program in Electrical and Computer Engineering. His faculty advisor is Sarah Koskie.

the primary method of attitude stabilization and magnetic torque coils as the method for momentum unloading. The LVLH referenced orientation of the spacecraft made earth horizon sensors a practical choice for sensing pitch and roll measurements. Likewise, a three-axis magnetometer would be used for measuring the yaw angle.

A novel mechanical and electrical design, developed for TEST, focused on the modularization of the major subsystems and instrumentation. Accordingly, the attitude control module, shown in Figure 2, was responsible for retrieving sensor data as well as relaying attitude commands from the attitude computer to the actuator hardware. The interface from the computer to this module was a standard RS485 bus with a backup I2C bus. Parallel connections were used for interfacing with the sensor and actuator peripherals using standard DSUB connectors. This configuration made integration simply a matter of “plug and play” and would allow for extensive system testing prior to integration. The configuration was also meant to be platform independent, allowing for extreme flexibility in choosing a flight computer.



Figure 2: Attitude Control Module

2 Coordinate Systems

The following sections provide an overview of the models developed to simulate the attitude system. These models are extremely dependent on the coordinate systems in which they are derived. For this reason, the various coordinate systems used in the development of these models are briefly discussed.

(1) The heliocentric coordinate frame is used for determining the vector pointing from the satellite center of mass to the center of the sun. The origin of this frame is defined to be the center of the sun. The z-axis is given by the vector pointing from the origin in the direction normal to the ecliptic plane. The x-axis is given by the vector pointing from the origin to the vernal equinox, and finally, the y-axis completes the

coordinate triad.

(2) The earth-fixed celestial coordinate frame is used for developing the equations of motion of the satellite orbit. The origin of this frame is defined to be the center of the earth. The z-axis is taken to be the rotational axis of the earth. The x-axis points from the origin to the vernal equinox, and finally, the y-axis completes the coordinate triad.

(3) The earth-fixed terrestrial coordinate frame is used in the determination of the earth’s main field magnetic flux vector in the geomagnetic model, which will be discussed later. Unlike the celestial coordinate frame, which was defined by a set of heavenly bodies, the terrestrial coordinate frame is defined by a set of fixed points on the earth-ellipsoid. Specifically, the x-axis points from the origin to the zero degree latitude/longitude point instead of the vernal equinox. Similar to the celestial coordinate frame, however, the z-axis aligns with the rotational axis and the y-axis completes the coordinate triad.

(4) The local-vertical/local-horizontal (LVLH) coordinate frame serves as the primary reference frame for the attitude system. The origin of this frame is defined as the satellite’s center of mass. The z-axis points from the origin in the direction parallel to the nadir. The y-axis points in the negative direction of the satellite orbital normal, and the x-axis completes the coordinate triad.

(5) The satellite coordinate frame is arbitrarily chosen according to various physical features of the satellite. For simplicity of calculation, the origin of the system was chosen to be the satellite’s center of mass and the coordinate axes were chosen to align with satellite principal axes.

3 Coordinate Transformations

When modeling the motion of a spacecraft, it is often necessary to transform the coordinates in one reference frame to the corresponding coordinates in another reference frame. If \mathbf{r} and \mathbf{r}' are equivalent vectors in two coordinate systems, then they are related by

$$\mathbf{r}' = \mathbf{A}\mathbf{r} + \mathbf{a}, \quad (1)$$

where \mathbf{A} is known as the direction cosine matrix and \mathbf{a} is some transformation of the origin. (For most applications $\mathbf{a} = 0$.) Because \mathbf{A} is an orthogonal matrix, its inverse is equivalent to its transpose. Mathematically, this is expressed as

$$\mathbf{A}^{-1} = \mathbf{A}^T. \quad (2)$$

The direction cosine matrix can be computed in several ways. The choice of method is most often dependent on the application. One of the simplest methods involves the matrix product of three successive rotations about the coordinate axes. The angles of rotation in this method are commonly referred to as the Euler angles. In this paper, the angles ϕ , θ , and ψ will be used to denote the Euler angles of rotation about the $\hat{\mathbf{x}}$, $\hat{\mathbf{y}}$, and $\hat{\mathbf{z}}$ axes respectively. The direction cosine matrices associated with these rotations are thus given by

$$\mathbf{A}_\phi = \begin{bmatrix} 1 & 0 & 0 \\ 0 & \cos \phi & \sin \phi \\ 0 & -\sin \phi & \cos \phi \end{bmatrix} \quad (3)$$

$$\mathbf{A}_\theta = \begin{bmatrix} \cos \theta & 0 & -\sin \theta \\ 0 & 1 & 0 \\ \sin \theta & 0 & \cos \theta \end{bmatrix} \quad (4)$$

$$\mathbf{A}_\psi = \begin{bmatrix} \cos \psi & \sin \psi & 0 \\ -\sin \psi & \cos \psi & 0 \\ 0 & 0 & 1 \end{bmatrix}. \quad (5)$$

Another method, sometimes referred to as the vector method, is useful when at least two vector quantities are known in both coordinate systems. Suppose \mathbf{u} and \mathbf{v} represent vector quantities in a given coordinate system. Then, the following orthogonal matrix is defined:

$$\mathbf{M} = [\hat{\mathbf{q}} \quad \hat{\mathbf{r}} \quad \hat{\mathbf{s}}], \quad (6)$$

where

$$\hat{\mathbf{q}} = \frac{\mathbf{u}}{|\mathbf{u}|} \quad (7)$$

$$\hat{\mathbf{r}} = \frac{\mathbf{u} \times \mathbf{v}}{|\mathbf{u} \times \mathbf{v}|} \quad (8)$$

$$\hat{\mathbf{s}} = \hat{\mathbf{q}} \times \hat{\mathbf{r}}. \quad (9)$$

Suppose now that \mathbf{u}' and \mathbf{v}' represent the equivalent vector quantities in a secondary coordinate system. Then a similar orthogonal matrix \mathbf{M}' is defined, and the direction cosine \mathbf{A} , representing the transformation from the first coordinate system to the second coordinate system, is given by

$$\mathbf{A} = \mathbf{M}'\mathbf{M}^T. \quad (10)$$

Another way to define a coordinate transformation is to use a quaternion representation. This representation is more compact than the direction cosine representation and is more convenient for computer operations. For these reasons it is often the representation of choice for attitude parameterization. Euler's theorem states that any rotation of a rigid body can be given by a rotation through some angle about some fixed axis. If the angle of rotation is denoted as Φ and the axis of

rotation is denoted by the unit vector $\hat{\mathbf{e}}$, then the elements of the quaternion are given by

$$q_1 = \hat{e}_1 \sin \frac{\Phi}{2} \quad (11)$$

$$q_2 = \hat{e}_2 \sin \frac{\Phi}{2} \quad (12)$$

$$q_3 = \hat{e}_3 \sin \frac{\Phi}{2} \quad (13)$$

$$q_4 = \cos \frac{\Phi}{2}. \quad (14)$$

The four quaternion elements defined above are not independent, but satisfy the equation

$$q_1^2 + q_2^2 + q_3^2 + q_4^2 = 1. \quad (15)$$

Letting $\mathbf{q} = [q_1 \quad q_2 \quad q_3]^T$, the direction cosine matrix can be expressed in terms of the quaternion by

$$\mathbf{A} = (q_4^2 - \mathbf{q}^2) \mathbf{1} + 2\mathbf{q}\mathbf{q}^T - 2q_4\mathbf{Q}, \quad (16)$$

where

$$\mathbf{Q} = \begin{bmatrix} 0 & -q_3 & q_2 \\ q_3 & 0 & -q_1 \\ -q_2 & q_1 & 0 \end{bmatrix}. \quad (17)$$

The transformation methods described above are sufficient for most of the work discussed in this paper with one major exception. Special care must be taken when transforming coordinates from the earth-fixed celestial frame to the earth-fixed terrestrial frame. This transformation is very complex and is beyond the scope of this paper. For a discussion of this transformation please refer to [3].

4 System Simulation

Computer simulation is needed for testing the attitude system. For this reason, several computer models were developed to simulate the spacecraft environment and attitude response. The simulator developed for the work discussed in this paper was created in Simulink and is shown below in Figure 3. The large block in the upper left corner of the Simulink block diagram labeled Orbital Data loads saved orbital and geomagnetic data from a file and incrementally provides this data to the rest of the models at each time step. (The data is computed separately using a Matlab script to save computational time.) From the top to bottom, the outputs of this block are the magnetic field vector in the LVLH frame, the vector pointing from the center of the sun to the satellite center of mass in the LVLH frame, the position and velocity vectors of the satellite in the earth-fixed terrestrial frame, and the position

and velocity vectors of the satellite in the earth-fixed celestial frame. The block immediately to the right of the orbital data block labeled Satellite Parameters contains a lists of constants which parameterize the satellite's physical features. The next block to the right of the satellite parameters block labeled Disturbance Model computes all external environmental torques on the satellite body. Below the satellite parameter block is the nonlinear plant model, which computes the attitude of satellite. The inputs to this model include the disturbance and control torques. From top to bottom, the outputs of this model are the attitude quaternion vector, the speeds of the reaction wheels, and the derivative of the attitude quaternion vector. The block directly below the plant labeled Controller is the reaction wheel controller. Finally, the block below the disturbance model labeled Fuzzy Controller represents the magnetic coil control system used for unloading the excess reaction wheel momentum. The attitude response of a typical run is given in the last plot of Figure 7. Please note that the scale on the y-axis of this plot is magnified 10000x's and that the discontinuities stem from violations in the simulation step size.

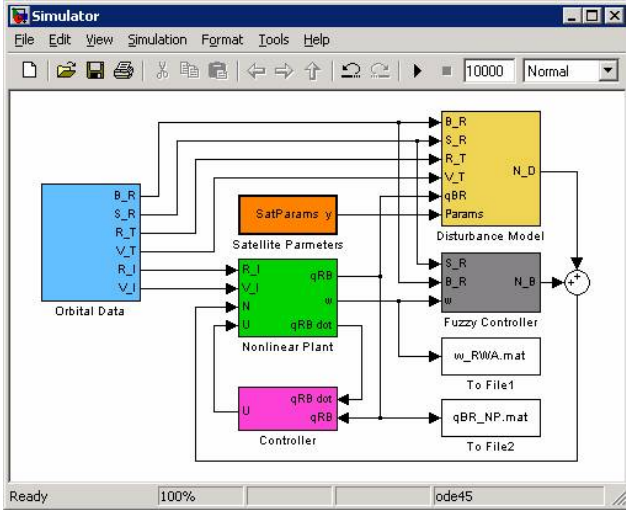


Figure 3: Attitude Simulator

Orbit Model

The orbit model, shown in Figure 4, was developed in Matlab using Newton's equation of motion for a particle under a central force.

The vectoral expression for Newton's equation is given by

$$m\ddot{\mathbf{r}} = f(r)\hat{\mathbf{e}}_r, \quad (18)$$

where \mathbf{r} and m are defined to be the position and mass of the particle respectively. Noting that the accelera-

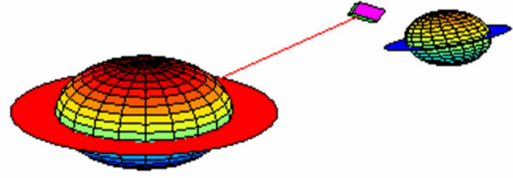


Figure 4: Orbit Simulation

tion term in the above equation can be expressed in polar coordinates as

$$\ddot{\mathbf{r}} = (\ddot{r} - r\dot{\theta}^2)\hat{\mathbf{e}}_r + (2\dot{r}\dot{\theta} + r\ddot{\theta})\hat{\mathbf{e}}_\theta, \quad (19)$$

the normal and tangential components of Newton's equation can be separated such that

$$m(\ddot{r} - r\dot{\theta}^2) = f(r) \quad (20)$$

$$m(2\dot{r}\dot{\theta} + r\ddot{\theta}) = 0. \quad (21)$$

The force $f(r)$ is given by the universal law of gravitation and is expressed as

$$f(r) = -G\frac{Mm}{r^2}, \quad (22)$$

where G is the gravitational constant, M is the mass of the earth, and m is the mass of the satellite. (Note the convention of using boldface letters to represent vectors or matrices and non-boldface letters to represent scalar magnitudes.) The above equations can be expressed as a system of first order differential equations. Letting $x_1 = r$, $x_2 = \dot{r}$, $x_3 = \theta$, and $x_4 = \dot{\theta}$, equations (20) and (21) can be recast as

$$\dot{x}_1 = x_2 \quad (23)$$

$$\dot{x}_2 = x_1x_4^2 - G\frac{M}{x_1^2} \quad (24)$$

$$\dot{x}_3 = x_4 \quad (25)$$

$$\dot{x}_4 = -2\frac{x_2x_4}{x_1}. \quad (26)$$

Using Matlab, the above equations can then be numerically integrated to produce sets of position and velocity vectors for the satellite over a specified period of time. The equations of motion for the earth's orbit about the sun can be similarly formulated and integrated to likewise produce sets of position and velocity vectors for the earth. The combined data can then be used to deduce the position and velocity vectors of the satellite relative to the sun.

It should be noted, however, that the above equations are only valid in an inertial coordinate system, i.e. the

earth-fixed celestial frame or the heliocentric frame. In order to obtain position, velocity, and sun-to-satellite vectors in a particular reference frame, transformations such as the ones described above must be performed on the calculated data.

Geomagnetic Model

A geomagnetic model is necessary for computing the components of the earth's main field magnetic flux vector for comparison with on board magnetometer measurements in the attitude determination algorithm as well as for environmental modeling. Such models are readily available in Fortran and C and can be downloaded from the National Geophysical Data Center website [7]. The development of these algorithms is beyond the scope of this paper and will not be discussed. It should be mentioned, however, that these models produce vectors with components resolved around the earth-fixed terrestrial coordinate frame. Thus, in order to use these models for comparison of data taken relative to another coordinate frame, transformations must be performed on the model outputs. For the purposes of this paper, a transformation between the earth-fixed terrestrial frame and the earth-fixed celestial frame was needed. The derivation of this transformation is also beyond the scope of this paper. Discussions of this transformation and several other useful transformations can be found in [3].

Disturbance Models

The attitude control system of any satellite must be capable of overcoming all external forces that might cause the satellite to stray from its objective attitude. Thus, when designing the attitude simulator all relevant disturbance torques must be considered, including the gravity gradient torque, the solar radiation torque, the aerodynamic friction torque, and the magnetic dipole torque. The following sections give a brief overview of the models used to simulate these torques.

Gravity Gradient Disturbance Model

The gravity gradient torque is caused by variation in the earth's gravitational force over the satellite body. If a spherical mass distribution is assumed for the earth, then the gravitational force acting on an elemental mass of the satellite body is given by

$$d\mathbf{F}_i = -\frac{\mu\mathbf{R}_i}{R_i^3}dm_i, \quad (27)$$

where $\mu = GM$ and \mathbf{R}_i is the vector pointing from the center of the earth to the elemental mass dm_i . Letting \mathbf{r}_i represent the vector from the satellite's center

of mass to the elemental mass, the differential torque about the satellite's center of mass due to the above force is then

$$d\mathbf{N}_i = -\frac{\mu}{R_i^3}(\mathbf{r}_i \times d\mathbf{R}_i)dm_i. \quad (28)$$

Let \mathbf{R}_i now be expressed as

$$\mathbf{R}_i = \mathbf{R}_s + \mathbf{r}_i, \quad (29)$$

where \mathbf{R}_s is the vector from the center of the earth to the satellite's center of mass. As shown in [1], the denominator of the above expression can then be expressed as

$$R_i^{-3} = R_s^{-3} \left[1 - \frac{3(\mathbf{R}_s \cdot \mathbf{r}_i)}{R_s^2} \right]. \quad (30)$$

Substituting the above equation into (28) and integrating gives the following expression for the torque about the satellite center of mass:

$$\begin{aligned} \mathbf{N}_{GG} = & -\frac{\mu}{R_s^3} \int (\mathbf{r}_i \times \mathbf{R}_s) dm_i \\ & + \frac{3\mu}{R_s^5} \int (\mathbf{R}_s \cdot \mathbf{r}_i)(\mathbf{R}_i \times \mathbf{R}_s) dm_i. \end{aligned} \quad (31)$$

Due to the symmetry of the problem, the first integral on the right hand side will drop out of the above equation, leaving only

$$\mathbf{N}_{GG} = \frac{3\mu}{R_s^5} \int (\mathbf{R}_s \cdot \mathbf{r}_i)(\mathbf{R}_i \times \mathbf{R}_s) dm_i. \quad (32)$$

For simplicity, assume now that all vectors in the above equation have been transformed to the satellite frame. After separating the above equation into component form, the symmetry argument then allows for the elimination of more terms, and the following expressions are left:

$$\mathbf{N}_{GGx} = \frac{3\mu}{R_s^5} R_{sy} R_{sz} (I_{zz} - I_{yy}) \quad (33)$$

$$\mathbf{N}_{GGy} = \frac{3\mu}{R_s^5} R_{sx} R_{sz} (I_{xx} - I_{zz}) \quad (34)$$

$$\mathbf{N}_{GGz} = \frac{3\mu}{R_s^5} R_{sx} R_{sy} (I_{yy} - I_{xx}), \quad (35)$$

where the components of the inertia tensor are given by

$$I_{xx} = \int (r_{iy}^2 + r_{iz}^2) dm_i \quad (36)$$

$$I_{yy} = \int (r_{ix}^2 + r_{iz}^2) dm_i \quad (37)$$

$$I_{zz} = \int (r_{ix}^2 + r_{iy}^2) dm_i. \quad (38)$$

The above equations can be written compactly in matrix notation as

$$\mathbf{N}_{GG} = \frac{3\mu}{R_s^5} [\mathbf{R}_s \times (\mathbf{I}\mathbf{R}_s)], \quad (39)$$

where \mathbf{I} is the inertia tensor given by

$$\mathbf{I} = \begin{bmatrix} I_{xx} & 0 & 0 \\ 0 & I_{yy} & 0 \\ 0 & 0 & I_{zz} \end{bmatrix}. \quad (40)$$

Solar Radiation Disturbance Model

In this section, the torque about the satellite's center of mass produced by incident solar radiation is considered. It is assumed that the solar radiation force on the satellite body is due to a combination of the radiation that is absorbed, reflected specularly, and reflected diffusely. Let P denote the momentum flux incident on an elemental area dA with unit normal $\hat{\mathbf{N}}$ such that

$$P = \frac{F_e}{c} \approx 4.5 \times 10^{-6} \text{ Kg}(ms)^{-1}, \quad (41)$$

where F_e is the mean integrated solar energy flux and c is the speed of light. The expression for the differential force on a given surface, with unit surface normal $\hat{\mathbf{N}}$, due to absorption is then given by

$$d\mathbf{F}_{Absorb} = -PC_a \cos(\theta) \hat{\mathbf{S}} dA, \quad (42)$$

where C_a is the absorption coefficient, $\hat{\mathbf{S}}$ is the unit vector pointing from the center of the sun to the satellite center of mass, and θ is the angle between $\hat{\mathbf{S}}$ and $\hat{\mathbf{N}}$ [1]. For computational models it is important to note that if the $\cos \theta$ term in the above expression and the expressions to follow is negative, it implies that the surface in question is not illuminated and thus no radiation force will result. The following expressions, taken from [1], give the necessary models for the forces caused by specularly and diffusely reflected radiation:

$$d\mathbf{F}_{Specular} = -2PC_s \cos^2(\theta) \hat{\mathbf{N}} dA \quad (43)$$

$$d\mathbf{F}_{Diffuse} = PC_d \left(-\frac{2}{3} \cos(\theta) \hat{\mathbf{N}} - \cos(\theta) \hat{\mathbf{S}} \right) dA, \quad (44)$$

where C_s is the coefficient of specular reflection and C_d is the coefficient of diffuse reflection. Considering all three sources, the total differential radiation force may be written as

$$\begin{aligned} d\mathbf{F}_{Total} = & -P \int (1 - C_s) \cos(\theta) \hat{\mathbf{S}} d\mathbf{A} \quad (45) \\ & - 2P \int \left(C_s \cos(\theta) + \frac{1}{3} C_d \right) \cos(\theta) \hat{\mathbf{N}} d\mathbf{A}, \end{aligned}$$

where $C_a + C_s + C_d = 1$. The torque about the satellite center of mass due to solar radiation over a given surface can thus be given as

$$\mathbf{N}_{Solar} = \int \mathbf{R} \times d\mathbf{F}_{total}, \quad (46)$$

where \mathbf{R} is the vector from the satellite center of mass to the elemental area $d\mathbf{A}$. Let \mathbf{F}_k denote the solar radiation force on a given geometrical surface of the spacecraft body such that

$$\mathbf{F}_k = \int d\mathbf{F}_{totalk}. \quad (47)$$

With this convention, it is possible to express the radiation torque as the sum of the torques caused by the radiation forces on the individual surface elements. Mathematically, this can be written as

$$\mathbf{N}_{Solar} = \sum \mathbf{R}_k \times \mathbf{F}_k, \quad (48)$$

where \mathbf{R}_k is the vector from the spacecraft center of mass to the center of pressure of the k^{th} surface element. Again, it should be noted that all vectors must be resolved about the satellite coordinate frame.

Aerodynamic Disturbance Model

For spacecraft in low-earth orbits, the aerodynamic disturbance torque is the strongest of the environmental disturbance torques. In this model it is assumed that the incident particle's energy is completely absorbed upon collision. The force $d\mathbf{f}_{Aero}$ on a surface element dA , with unit normal $\hat{\mathbf{N}}$, due to aerodynamic friction is thus given by

$$d\mathbf{f}_{Aero} = -\frac{1}{2} C_D \rho V^2 (\hat{\mathbf{N}} \cdot \hat{\mathbf{V}}) \hat{\mathbf{V}} dA, \quad (49)$$

where C_D is the drag coefficient, ρ is the atmospheric density, and \mathbf{V} is the translational velocity of the elemental mass dA . Accordingly, the aerodynamic disturbance torque about the satellite center of mass is given by

$$\mathbf{N}_{Aero} = \int \mathbf{r}_i \times d\mathbf{f}_{Aero}, \quad (50)$$

where \mathbf{r}_i is the vector from the spacecraft center of mass to the surface element dA . The above integral is valid over all surfaces for which $\hat{\mathbf{N}} \cdot \hat{\mathbf{V}} > 0$ holds. Consider now that the translational velocity of the surface element dA may be written in terms of the satellite angular velocity ω and the velocity of the satellite center of mass \mathbf{V}_0 as

$$\mathbf{V} = \mathbf{V}_0 + \omega \times \mathbf{r}_i. \quad (51)$$

It is important to note at this point that the translational velocity \mathbf{V} is relative to the atmosphere of the earth, which rotates at approximately the same rate as the earth itself. Computation of the aerodynamic disturbance force should thus be done in the earth-fixed terrestrial frame with the results transformed to the satellite frame. Now then, substituting (49) and (51) into (50) and neglecting all second-order terms in ω gives the following expression for the total aerodynamic friction torque

$$\begin{aligned} \mathbf{N}_{Aero} = & \frac{1}{2}C_D\rho V^2 \int (\hat{\mathbf{N}} \cdot \hat{\mathbf{V}}_0) dA \\ & + \frac{1}{2}C_D\rho V_0 \int \hat{\mathbf{N}} \cdot (\omega \times \mathbf{r}_i)(\hat{\mathbf{V}}_0 \times \mathbf{r}_i) dA \\ & + \frac{1}{2}C_D\rho V_0 \int (\hat{\mathbf{N}} \cdot \hat{\mathbf{V}}_0) [(\omega \times \mathbf{r}_i) \times \mathbf{r}_i] dA. \end{aligned} \quad (52)$$

Note that for spacecraft with $\omega r \ll V_0$ the second and third terms in the above equation are much smaller than the first and may be neglected. The above integral may also be decomposed into the vector sum of the integrals over the individual spacecraft shapes as discussed in the above section for the solar radiation torque.

Magnetic Disturbance Model

The primary sources of magnetic disturbance are the spacecraft magnetic moments, eddy currents, and hysteresis. Magnetic disturbance from the satellite magnetic moments is most often the strongest of the three and is the only magnetic disturbance considered in this paper. This torque is given by the expression

$$\mathbf{N}_{mag} = \mathbf{M} \times \mathbf{B}, \quad (53)$$

where \mathbf{M} is the sum of the individual magnetic moments and \mathbf{B} is the geomagnetic flux density. Note that for simulations using geomagnetic models \mathbf{B} must be transformed from the earth-fixed terrestrial frame to the satellite frame.

Dynamics Model

When applied to a rigid body spacecraft, the most fundamental tool for quantifying rotational motion is angular momentum. Consider a rigid body spacecraft moving in an inertial coordinate system. Representing the spacecraft as a collection of particles, the spacecraft angular momentum is given by

$$\mathbf{L} = \sum \mathbf{R}_i \times m_i \mathbf{V}_i, \quad (54)$$

where \mathbf{R}_i is the vector pointing from the origin of the inertial frame to the element of mass m_i and \mathbf{V}_i is its

first time derivative. Now let

$$\mathbf{R}_i = \mathbf{R}_s + \mathbf{r}_i, \quad (55)$$

where \mathbf{R}_s is the vector from the origin to the satellite center of mass and \mathbf{r}_i is the vector from the center of mass to the element of mass m_i . The angular momentum of the spacecraft body may then be rewritten as

$$\mathbf{L} = \sum (\mathbf{R}_s + \mathbf{r}_i) \times m_i (\mathbf{V}_s + \dot{\mathbf{r}}_i). \quad (56)$$

Expanding the expression above and noting that $\sum m_i \mathbf{r}_i = 0$, it can be shown that

$$\mathbf{L} = M\mathbf{R}_s \times \mathbf{V}_s + \sum (m_i \mathbf{r}_i \times \dot{\mathbf{r}}_i), \quad (57)$$

where the first term on the right represents the angular momentum of the satellite considered as a point with mass M and the second term represents the angular momentum of the satellite about its center of mass. Owing to the nature of the attitude problem, only the second term is considered, leaving

$$\mathbf{L} = \sum (m_i \mathbf{r}_i \times \dot{\mathbf{r}}_i). \quad (58)$$

It is important to note that in the above expression $\dot{\mathbf{r}}_i \neq 0$. This is because the above momentum equations were derived in an inertial reference frame where Newton's laws of motion are valid and not in the satellite reference frame where Newton's laws of motion are invalid. Let \mathbf{r}_i now denote the position vector of the i^{th} particle with respect to the earth-fixed celestial frame and \mathbf{r}'_i the position vector of the i^{th} particle with respect to the satellite frame. There then exists a transformation \mathbf{A} such that

$$\mathbf{r}'_i = \mathbf{A} \mathbf{r}_i \quad (59)$$

and

$$\frac{d\mathbf{r}'_i}{dt} = \frac{d\mathbf{A}}{dt} \mathbf{r}_i + \mathbf{A} \frac{d\mathbf{r}_i}{dt}. \quad (60)$$

As shown in [1], the derivative in the first term on the right hand side of the above equation is given by

$$\frac{d\mathbf{A}}{dt} = \boldsymbol{\Omega}' \mathbf{A}(t), \quad (61)$$

where

$$\boldsymbol{\Omega}' = \begin{bmatrix} 0 & \omega_w & -\omega_v \\ -\omega_w & 0 & \omega_u \\ \omega_v & -\omega_u & 0 \end{bmatrix}. \quad (62)$$

Plugging the above expression into (60) and noting that $d\mathbf{r}'_i/dt = 0$, then gives

$$(\dot{\mathbf{r}}_i)_{sat} = -\boldsymbol{\Omega}' \mathbf{A}(t) \mathbf{r}_i = \omega \times (\mathbf{r}_i)_{sat}, \quad (63)$$

where ω is the instantaneous angular velocity of the satellite with respect to earth-fixed celestial frame, but with components resolved along the satellite frame. Note the subscripts in the above expression, which indicate that the corresponding vectors originally resolved along the inertial frame are now taken with respect to the satellite frame. Substituting the above expression into (58) now leads to following result for the angular momentum of the satellite about its center of mass, with all vector components measured relative to the satellite frame:

$$\mathbf{L} = \sum [m_i \mathbf{r}_i \times (\omega \times \mathbf{r}_i)]. \quad (64)$$

Expanding the above expression into component form yields

$$L_x = \sum (m_i [r_i^2 \omega_x - (\mathbf{r}_i \cdot \omega) r_{ix}]) \quad (65)$$

$$L_y = \sum (m_i [r_i^2 \omega_y - (\mathbf{r}_i \cdot \omega) r_{iy}]) \quad (66)$$

$$L_z = \sum (m_i [r_i^2 \omega_z - (\mathbf{r}_i \cdot \omega) r_{iz}]). \quad (67)$$

Recalling that the principal axes were chosen as the coordinate axes of the satellite frame and the definition of the inertia tensor given in (40), the vectorial equation of angular momentum finally reduces to

$$\mathbf{L} = \mathbf{I}\omega. \quad (68)$$

Similar to equations (59) and (60), the transformation from \mathbf{L} to \mathbf{L}' is given by

$$\mathbf{L}' = \mathbf{A}\mathbf{L}, \quad (69)$$

with first derivative given by

$$\frac{d\mathbf{L}'}{dt} = \frac{d\mathbf{A}}{dt}\mathbf{L} + \mathbf{A}\frac{d\mathbf{L}}{dt}, \quad (70)$$

where \mathbf{L} represents the angular momentum of the satellite with components resolved about the earth-fixed celestial frame and \mathbf{L}' represents the angular momentum of the satellite with components resolved about the satellite frame. Substituting (61) into the expression above and rearranging then leads to

$$(\dot{\mathbf{L}})_{sat} = \mathbf{N} = \mathbf{I}\dot{\omega} + \omega \times (\mathbf{L})_{sat}, \quad (71)$$

where all vectors are taken with respect to the satellite frame and \mathbf{N} is the sum of the external torques applied to the satellite. Note that the above expression was derived for a rigid body. A satellite with reaction wheels cannot be taken as a strict rigid body. Fortunately, the above equation can be easily modified to account for the angular momentum created by a reaction wheel assembly. Let

$$\mathbf{L}_{sat} = \mathbf{I}\omega + \mathbf{h}, \quad (72)$$

where \mathbf{h} is the net angular momentum due to the reaction wheel assembly. Then, (71) can be reformulated as

$$\mathbf{N} = \mathbf{I}\frac{d\omega}{dt} + \frac{d\mathbf{h}}{dt} + \omega \times (\mathbf{I}\omega + \mathbf{h}), \quad (73)$$

where once again all vectors are assumed to be resolved about the satellite frame. Now when combined with the kinematic equations of motion, the above expression completely specifies the attitude of a satellite with reaction wheel control. As derived in [1], the kinematic equations of motion for the quaternion attitude parameterization are given by

$$\dot{\mathbf{q}} = \frac{1}{2}\mathbf{\Omega}\mathbf{q}, \quad (74)$$

where

$$\mathbf{\Omega} = \begin{bmatrix} 0 & \omega_z & -\omega_y & \omega_x \\ -\omega_z & 0 & \omega_x & \omega_y \\ \omega_y & -\omega_x & 0 & \omega_z \\ -\omega_x & -\omega_y & -\omega_z & 0 \end{bmatrix}. \quad (75)$$

5 Plant Linearization

The nonlinear equations of attitude motion derived above are not ideal for controller synthesis. In order to take advantage of linear control techniques, a linear approximation of the above equations must be found. Expanding (73) into component form gives the following system of equations

$$N_x = I_{xx}\dot{\omega}_x + \dot{h}_x + \omega_y\omega_z(I_{zz} - I_{yy}) + \omega_y h_z - \omega_z h_y \quad (76)$$

$$N_y = I_{yy}\dot{\omega}_y + \dot{h}_y + \omega_x\omega_z(I_{xx} - I_{zz}) + \omega_z h_x - \omega_x h_z \quad (77)$$

$$N_z = I_{zz}\dot{\omega}_z + \dot{h}_z + \omega_x\omega_y(I_{yy} - I_{xx}) + \omega_x h_y - \omega_y h_x. \quad (78)$$

Note that in the equations above ω specifies the angular velocity of the satellite frame with respect to the earth-fixed celestial frame. For simplicity, the earth-fixed celestial frame will now be referred to as the inertial frame. Similarly, the LVLH frame will be referred to as the reference frame and the satellite frame will be referred to as the body frame. With this in mind, the angular velocity term in the equations above may now be given as

$$\omega_{BI} = \omega_{BR} + \omega_{RI}, \quad (79)$$

where ω_{BI} is the angular velocity of the body frame with respect to the inertial frame, ω_{BR} is the angular

velocity of the body frame with respect to the reference frame, and ω_{RI} is the angular velocity of the reference frame with respect to the inertial frame. Note now that ω_{RI} is conveniently expressed in terms of the orbital angular velocity, with vector components in the body frame, as

$$\omega_{RI} = \mathbf{A}_{BR} \begin{bmatrix} 0 \\ -\omega_0 \\ 0 \end{bmatrix}, \quad (80)$$

where \mathbf{A}_{BR} is the transformation from the reference frame to the body frame and ω_0 is the magnitude of the orbital angular velocity. In order to use small angle approximations, let the direction cosine matrix \mathbf{A}_{BR} be given in terms of the Euler angles as the matrix product of three consecutive rotations about the z , y , and x axes such that

$$\mathbf{A}_{BR} = \mathbf{A}_\phi \mathbf{A}_\theta \mathbf{A}_\psi, \quad (81)$$

where \mathbf{A}_ϕ , \mathbf{A}_θ , and \mathbf{A}_ψ were previously defined by (3), (4), and (5). For small angles ϕ , θ , and ψ , ω_{BI} is then approximately given by

$$\omega_{BI} = \begin{bmatrix} \dot{\phi} - \psi\omega_0 \\ \dot{\theta} - \omega_0 \\ \dot{\psi} + \phi\omega_0 \end{bmatrix}, \quad (82)$$

with vector components measured in the body frame. Returning to the nonlinear attitude equations of motion above, let \mathbf{N} now be given by the sum

$$\mathbf{N} = \mathbf{N}_{GG} + \mathbf{N}_D, \quad (83)$$

where \mathbf{N}_{GG} is the gravity gradient torque and \mathbf{N}_D accounts for all other disturbance torques. Recall that the components of the gravity gradient torque were given by (33), (34), and (35). Maintaining the small angle approximations and transforming to the body frame, the components of the gravity gradient torque may now be given as

$$\mathbf{N}_{GGx} \approx \frac{3\mu}{R_s^3} (I_{zz} - I_{yy})\phi \quad (84)$$

$$\mathbf{N}_{GGy} \approx \frac{3\mu}{R_s^3} (I_{xx} - I_{zz})\theta \quad (85)$$

$$\mathbf{N}_{GGz} \approx 0. \quad (86)$$

If a circular orbit is assumed, the above equations will further simplify to

$$\mathbf{N}_{GGx} \approx 3\omega_0^2 (I_{zz} - I_{yy})\phi \quad (87)$$

$$\mathbf{N}_{GGy} \approx 3\omega_0^2 (I_{xx} - I_{zz})\theta \quad (88)$$

$$\mathbf{N}_{GGz} \approx 0. \quad (89)$$

Substituting (82) and (83), with the gravity gradient torque as given above, into (76), (77), and (78) and neglecting higher order terms then finally leads to the following linear equations of motion:

$$I_{xx}\ddot{\phi} = (\omega_0 h_y - a)\phi - h_z \dot{\theta} + (h_y + b)\dot{\psi} \quad (90)$$

$$+ N_x - \dot{h}_x + \omega_0 h_z$$

$$I_{yy}\ddot{\theta} = -\omega_0 h_x \phi + h_z \dot{\phi} + c\theta - \omega_0 h_z \psi - h_x \dot{\psi} \quad (91)$$

$$+ N_y - \dot{h}_y$$

$$I_{zz}\ddot{\psi} = -(h_y + b)\dot{\phi} + h_x \dot{\theta} + (\omega_0 h_y + d)\psi \quad (92)$$

$$+ N_z - \dot{h}_z - \omega_0 h_x,$$

where

$$a = 4\omega_0^2 (I_{yy} - I_{zz}) \quad (93)$$

$$b = \omega_0 (I_{xx} - I_{yy} + I_{zz}) \quad (94)$$

$$c = 3\omega_0^2 (I_{zz} - I_{xx}) \quad (95)$$

$$d = \omega_0^2 (I_{xx} - I_{yy}). \quad (96)$$

6 Parametric Uncertainty

In the previous section, the nonlinear attitude equations of motion were linearized with respect to the Euler angles ϕ , θ , and ψ . The remaining system is still time-varying, however, by the inclusion of the reaction wheel momentum terms h_x , h_y , and h_z . Furthermore, in practice it is unlikely that the satellite inertia terms I_{xx} , I_{yy} , and I_{zz} are actually known. Thus it must be ensured that the controller not only stabilizes the nominal plant, but that it also robustly stabilizes all plant transfer functions within the range of uncertainty. In order to apply robust control theory to the uncertain, linear time-varying (LTV) system, the model will now be recast as a nominal linear time-invariant (LTI) system perturbed by some structured block diagonal uncertainty Δ . A multiplicative uncertainty model of the general form

$$\mathbf{\Pi} = (\mathbf{I} + \mathbf{W}_1 \Delta \mathbf{W}_2) \mathbf{P} \quad (97)$$

may be chosen to model the parametric uncertainty in the satellite inertia terms, where \mathbf{P} is the nominal value of the uncertain parameter. If the reaction wheels operate at zero momentum, the above multiplicative uncertainty model cannot be used to model the reaction wheel uncertainty. Instead an additive uncertainty model of the general form

$$\mathbf{\Pi} = \mathbf{P} + \mathbf{W}_1 \Delta \mathbf{W}_2 \quad (98)$$

must be used. If, however, the reaction wheels operate at a nonzero momentum, it is possible to use

multiplicative uncertainty for both the inertia terms and the reaction wheel momenta. Expressing the inertia and wheel momenta terms as uncertain parameters, the system model may now conveniently be formulated in a linear fractional transformation (LFT) framework as depicted below.

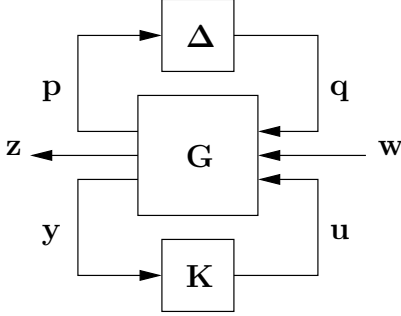


Figure 5: LFT Diagram

In Figure 5, \mathbf{G} represents the nominal plant with fixed reaction wheel angular momentum $\hat{\mathbf{h}}$ and inertia matrix \mathbf{I} , Δ represents the structured block diagonal uncertainty associated with \mathbf{h} and \mathbf{I} , and \mathbf{K} represents the control law discussed in the following section. The process of transforming a given model to a matrix LFT is often referred to as “pulling out the Δ ’s”. For systems as complex as the one under discussion this can be a rather tedious task. The burden is lessened, however, by using software packages such as Matlab.

7 Robust Controller Synthesis

Supposes that the controller \mathbf{K} is brought into the nominal plant \mathbf{G} in Figure 5 such that $\mathbf{M} = \underline{S}(\mathbf{G}, \mathbf{K})$. This transfer function is sometimes referred to as the lower star product. Assuming \mathbf{M} is a causal, bounded LTI operator, then the following conditions are equivalent:

- (i) *The uncertain system (M_{11}, Δ) is robustly stable.*
- (ii) *The inequality $\inf_{\Theta \in \Theta_a} \|\Theta M_{11} \Theta^{-1}\| < 1$ holds;*

where

$$\Delta = \{\text{diag}(\Delta_1, \dots, \Delta_d) : \Delta_k \in \mathcal{L}(L_2), \Delta_k \text{ causal}, \|\Delta_k\| \leq 1\}$$

and Θ_a is the commutant set corresponding to Δ [5]. The above result states that the robust synthesis for the setup in Figure 5 can be obtained by finding the infimum of

$$\|\Theta \underline{S}(\mathbf{G}, \mathbf{K}) \Theta^{-1}\|, \quad (99)$$

where \mathbf{K} ranges over the stabilizing class of controllers and Θ ranges over the commutant set of constant matrices Θ_a . In general this is not solvable by convex, finite dimensional methods. Thus heuristic algorithms must be considered. The most common method, termed *D-K iteration*, splits the problem into two steps: (1) synthesize an H_∞ controller; and (2) find a scaling that infimizes a scaled gain. Matlab’s Robust Toolbox provides several useful routines to implement such algorithms.

Considering the TEST Nanosatellite as an example case, Figure 6 gives the structured singular value plot associated with the closed loop system consisting of the uncertain plant and synthesized H_∞ controller. For this example, a 10% uncertainty was assumed for the inertia terms I_{xx} , I_{yy} , and I_{zz} . Likewise, the reaction wheels were allowed to vary within a range of 0 to 10000 rpms. The dimensions and mass of the satellite are $0.3 \text{ m} \times 0.3 \text{ m} \times 0.45 \text{ m}$ and 30 Kg . Finally, the radius and mass of each wheel is 0.04 m and 1 Kg . As can be seen from the plot, robust stability is guaranteed over the entire range of uncertainty.

8 Magnetic Unloading of the Wheels

External disturbance torques on the body of the satellite will inevitably result in reaction wheel saturation if a greater counter torque is not applied. For satellites in low-earth orbits, magnetic torque rods or coils are often used, which interact with the earth’s magnetic field to produce a torque about the spacecraft body. The basic control law for momentum unloading is given by

$$\mathbf{T} = -k\Delta\mathbf{h} = \mathbf{M} \times \mathbf{B}, \quad (100)$$

where k is the unloading control gain, $\Delta\mathbf{h}$ is the difference between the actual wheel momentum and the nominal wheel momentum, \mathbf{M} is the magnetic moment produced by the electromagnetic device, and \mathbf{B} is the magnetic field vector at the satellite coordinates. Recall that the torque due to the sum of the satellite magnetic moments was given by $\mathbf{N} = \mathbf{M} \times \mathbf{B}$. Therefore,

$$-k\Delta\mathbf{h} = \mathbf{M} \times \mathbf{B}. \quad (101)$$

Notice, however, that the moment vector \mathbf{M} cannot be computed from the above equation. Using the vector product by \mathbf{B} on both sides, the above equation becomes

$$\begin{aligned} \mathbf{B} \times (-k\Delta\mathbf{h}) &= \mathbf{B} \times (\mathbf{M} \times \mathbf{B}) \\ &= B^2\mathbf{M} - \mathbf{B}(\mathbf{M} \cdot \mathbf{B}). \end{aligned} \quad (102)$$

Assuming now that \mathbf{M} is perpendicular to \mathbf{B} , a non-general solution for \mathbf{M} is given by

$$\mathbf{M} = -\frac{k}{B^2}(\mathbf{B} \times \Delta\mathbf{h}). \quad (103)$$

Plugging the above value for \mathbf{M} into the control torque law gives the following expression for the torque produced by the interaction of the electromagnetic device with the earth's magnetic field:

$$\mathbf{T} = \mathbf{M} \times \mathbf{B} = -\frac{k}{B^2}[B^2\Delta\mathbf{h} - \mathbf{B}(\mathbf{B} \cdot \Delta\mathbf{h})]. \quad (104)$$

9 Fuzzy Gain-Scheduler

The control system described above for the magnetic unloading of the reaction wheels is also time-varying, because the components of the magnetic field are time-varying with respect to the satellite frame. Thus, the control gain must be chosen in such a way that the system maintains robustness over the variation in the magnetic flux orientation. In this case, robustness implies that the wheels are guaranteed not to saturate at any point over the lifetime of the spacecraft. Typically this would mean searching for a constant gain, via simulation, that would produce satisfactory results for several orbits. A constant gain solution does not take advantage of ideal unloading conditions, however, and worse yet could result in unnecessarily loading down the power system during the execution of critical satellite functions, such as transmitting data to the ground station. Thus, a gain-scheduler should be utilized to maximize efficient use of the available resources. Fuzzy logic provides a convenient method for performing this task.

A Mamdani-type fuzzy controller may be used to weight the magnetic unloading control gain. As an example, consider a fuzzy system with two inputs and a single output. Suppose now that the first and second inputs give measures on the relative orientations of the unit magnetic flux vector $\hat{\mathbf{B}}$ and the unit sun vector $\hat{\mathbf{S}}$, where $\hat{\mathbf{S}}$ points from the spacecraft to the sun. Mathematically, these inputs can be given as

$$u_1 = |\hat{\mathbf{B}} \times \hat{\Delta\mathbf{h}}| \quad (105)$$

$$u_2 = \sum \hat{\mathbf{S}} \cdot \hat{\mathbf{N}}_k, \quad (106)$$

where $\hat{\mathbf{N}}_k$ is the unit surface normal of the k^{th} solar array. (Note that for computer simulations, $\hat{\mathbf{S}} \cdot \hat{\mathbf{N}}_k < 0$ implies that the solar array is not illuminated and should be given a value of zero.) The choice of these inputs is meant to exploit the available torque and power resources of the satellite. Other inputs could also be

chosen based on the specific requirements of the satellite.

Assume now that three evenly distributed fuzzy membership functions are defined for each of the chosen input variables and five evenly distributed fuzzy membership functions are defined for the output gain value k . Accordingly, the fuzzy rules may be given as

- R1: If u_1 is low and u_2 is low, then k is very low.
- R2: If u_1 is low and u_2 is med, then k is very low.
- R3: If u_1 is low and u_2 is high, then k is med.
- R4: If u_1 is med and u_2 is low, then k is very low.
- R5: If u_1 is med and u_2 is med, then k is very low.
- R6: If u_1 is med and u_2 is high, then k is high.
- R7: If u_1 is high and u_2 is low, then k is med.
- R8: If u_1 is high and u_2 is med, then k is high.
- R9: If u_1 is high and u_2 is high, then k is very high.

Finally, assume a centroid defuzzification of the form

$$k = \frac{\int x_i \mu(x_i)}{\int \mu(x_i)}, \quad (107)$$

where $\mu(x_i)$ is the membership value associated with the element x_i . The system described above will result in a gain-scheduler that will yield high control gains at opportune times, low control gains at inopportune times, and intermediate control gains at times where the fuzzy rules conflict.

Considering the TEST Nanosatellite again as an example, the first two plots in Figure 7 show the implementation results for the fuzzy gain-scheduler discussed above. The first plot shows the inputs and output of the fuzzy system and the second plot gives the gives speeds of the reaction wheels in rpms. The simulation was conducted over several orbits to ensure that all periodicities were accounted for. Note that the wheel speeds stay within the range of 0 to 1000 rpms.

10 Conclusion

In this paper, the difficulties of ensuring the robust performance of a nominal linear plant perturbed by parametric uncertainty and the formulation of an optimal magnetic wheel unloading strategy were discussed. First, the problem was formulated addressing the specific requirements for simulating the spacecraft environment and attitude response. Mathematical models were developed for the satellite orbital motion, the external attitude disturbances, and the dynamic attitude response. Second, a linearization of the nonlinear equations of attitude dynamics was presented with respect to the nominal spacecraft attitude. The resulting LTV system was then recast as an LFT, by a process known

as “pulling out the delta’s”, to separate the parametric uncertainty from the nominal LTI plant equations. Next, a strategy for robust controller synthesis was provided and the results for the TEST Nanosatellite example were presented. Finally, the control law for magnetic wheel unloading was given with a description of a fuzzy gain-scheduler. Results for the fuzzy system were also presented for the TEST Nanosatellite example.

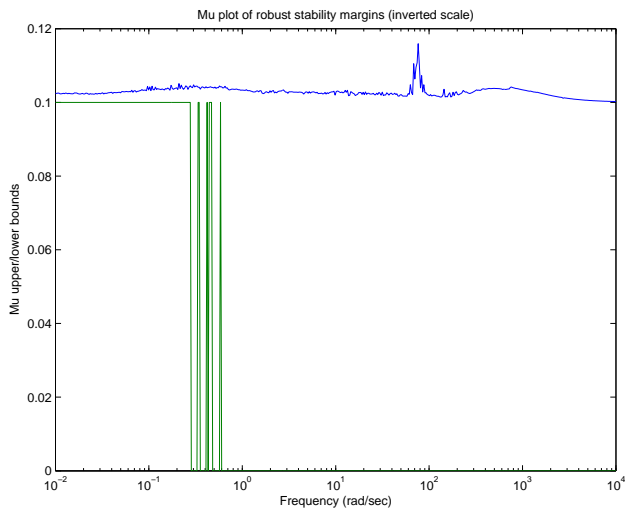


Figure 6: μ Plot

References

- [1] Wertz, James R., ed. *Spacecraft Attitude Determination and Control*. Cambridge University Press, Dordrecht, Boston, London, 1978.
- [2] Sidi, Marcel J. *Spacecraft Dynamics and Control*. Cambridge University Press, 1997.
- [3] Vallado, David A. *Fundamentals of Astrodynamics and Applications*. Microcosm Press, Dordrecht, Boston, London, 2001.
- [4] Zhou, Kemin *Essentials of Robust Control*. Prentice Hall, Upper Saddle River, New Jersey, 1998.
- [5] Dullerud, Geir E. *A Course in Robust Control Theory: A Convex Approach*. Springer, 2000.
- [6] Voss, David L.; et. al. “A Highly Modular Nanosatellite: TEST”. 18th Annual AIAA/USU Conference on Small Satellites, Logon, UT, August 2004. SSC01-VIII-6
- [7] McLean, Susan *Geomagnetic Models and Software*. 4 April 2005. National Geophysical Data Center. <http://www.ngdc.noaa.gov/seg/geomag/models.shtml> 2 May 2005.

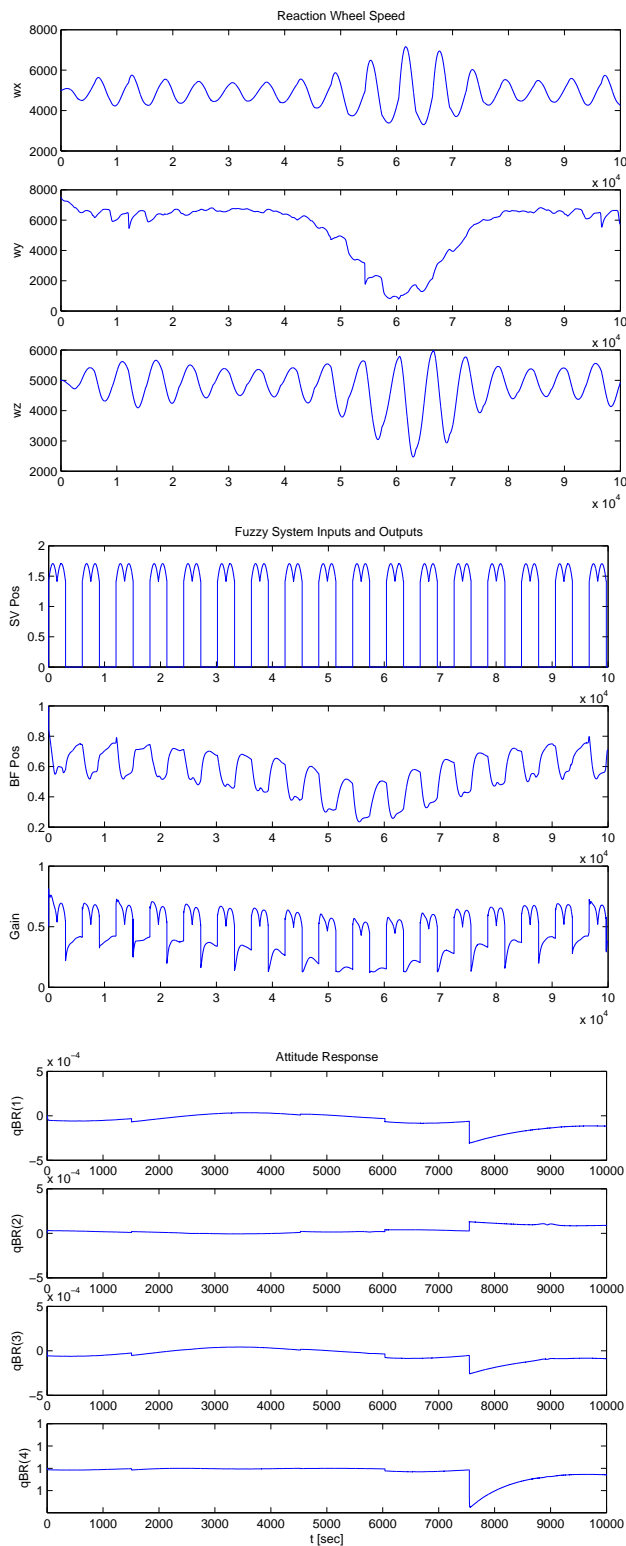


Figure 7: Results